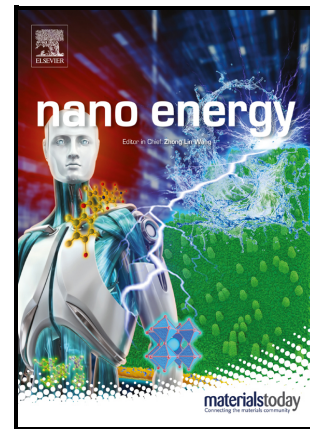


Promoting Maturation and Contractile Function of Neonatal Rat Cardiomyocytes by Self-powered Implantable Triboelectric Nanogenerator

Luming Zhao, Zhongbao Gao, Wei Liu, Chunlan Wang, Dan Luo, Shengyu Chao, Siwei Li, Zhou Li, Changyong Wang, Jin Zhou



PII: S2211-2855(22)00875-8

DOI: <https://doi.org/10.1016/j.nanoen.2022.107798>

Reference: NANOEN107798

To appear in: *Nano Energy*

Received date: 3 July 2022

Revised date: 20 August 2022

Accepted date: 8 September 2022

Please cite this article as: Luming Zhao, Zhongbao Gao, Wei Liu, Chunlan Wang, Dan Luo, Shengyu Chao, Siwei Li, Zhou Li, Changyong Wang and Jin Zhou, Promoting Maturation and Contractile Function of Neonatal Rat Cardiomyocytes by Self-powered Implantable Triboelectric Nanogenerator, *Nano Energy*, (2022) doi:<https://doi.org/10.1016/j.nanoen.2022.107798>

This is a PDF file of an article that has undergone enhancements after acceptance, such as the addition of a cover page and metadata, and formatting for readability, but it is not yet the definitive version of record. This version will undergo additional copyediting, typesetting and review before it is published in its final form, but we are providing this version to give early visibility of the article. Please note that, during the production process, errors may be discovered which could affect the content, and all legal disclaimers that apply to the journal pertain.

© 2022 Published by Elsevier.

Promoting Maturation and Contractile Function of Neonatal Rat Cardiomyocytes by Self-powered Implantable Triboelectric Nanogenerator

Luming Zhao ^{a,1}, Zhongbao Gao ^{a,1}, Wei Liu ^a, Chunlan Wang ^a, Dan Luo ^{b,c}, Shengyu Chao ^{b,c}, Siwei Li ^a, Zhou Li ^{b,c,d,*}, Changyong Wang ^{a,*}, Jin Zhou ^{a,*}

^a Beijing Institute of Basic Medical Sciences, 27 Taiping Rd, Beijing 100850, PR China

^b Beijing Institute of Nanoenergy and Nanosystems, Chinese Academy of Sciences, Beijing 101400, China

^c School of Nanoscience and Technology, University of Chinese Academy of Sciences, Beijing 100049, China

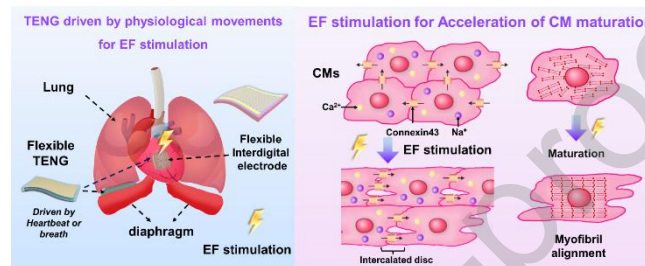
^d Center on Nanoenergy Research, School of Chemistry and Chemical Engineering, School of Physical Science and Technology, Guangxi University, Nanning 530004, China

Corresponding authors: Zhou Li (zli@binn.cas.cn), Changyong Wang (wcy2000_zm@163.com), and Jin Zhou (sisun819@outlook.com).

Abstract: Cardiomyocyte-based therapeutic strategy is a promising approach to treat myocardial injury; however, the prognostic power of this approach is currently limited by the immaturity of cardiomyocytes. Here, a flexible self-powered implantable electrical stimulator based on the triboelectric nanogenerator (TENG) was proposed to induce the maturation of cardiomyocytes by generating an electric field on the interdigitated electrode. The results showed that the TENG-based self-powered stimulator significantly promoted the maturation of neonatal rat cardiomyocytes (NRCMs) *in vitro* by increasing the expression of connexin 43, α -actinin, and c-troponin T. In addition, electrical stimulation also improved sarcomere organization and fracture formation, and significantly increased the intracellular Ca^{2+} levels, Ca^{2+} transient rate, and Ca^{2+} peak amplitudes of cardiomyocytes. TENG was also shown to

be driven by the breath of rats and the heartbeat of rabbits, suggesting it could be used as an implantable medical electronic device for electrically promoting the maturation of neonatal cardiomyocytes. This work develops a TENG-based self-powered implantable medical device, which provides important technical support for clinical treatment of myocardial defects and restoration of the physiological function of cardiac tissue.

Graphical Abstract



In this work, a flexible self-powered implantable electrical stimulator based on the triboelectric nanogenerator (TENG) was proposed to induce the maturation of cardiomyocytes by generating an electric field on the interdigitated electrode. The results showed that TENG-based self-powered stimulator significantly promoted the maturation of neonatal rat cardiomyocytes (NRCMs) *in vitro* by increasing the expression of connexin 43, α -actinin, and c-troponin T. In addition, electrical stimulation also improved sarcomere organization and fracture formation, and significantly increased the intracellular Ca^{2+} levels, Ca^{2+} transient rate, and Ca^{2+} peak amplitudes of cardiomyocytes. TENG was also shown to be driven by the daily breathing of rats and the heartbeat of rabbits, suggesting it could be used as an implantable medical electronic device for electrically promoting the maturation of neonatal cardiomyocytes. This work develops a TENG-based self-powered implantable medical device, which provides important technical support for clinical treatment of myocardial defects and restoration of the physiological function of cardiac tissue.

Keywords: Triboelectric nanogenerator, Electrical stimulation, neonatal rat

cardiomyocytes, maturation

1. Introduction

Myocardial injury, which can be caused by myocarditis, cardiotoxic drugs and myocardial infarction, is a serious disease that threatens public health [1, 2]. Clinically, myocardial injury can lead to cardiac insufficiency. In severe cases, it can lead to heart failure and even death [3, 4]. Heart transplant is the ultimate treatment for heart failure, but is limited by the lack of organ donors and immunosuppressive therapy [5]. Therefore, exploring effective alternatives to repair damaged cardiac tissue has become an urgent and significant problem in the current cardiovascular treatment.

Recently, cardiomyocytes-based therapeutic strategies have been used to treat heart failure and restore lost myocardium [6-9]. However, cardiomyocytes grow as single cells with a functionally and structurally mature phenotype and hardly proliferate after birth [10, 11], which limits the development of cardiomyocyte-based therapeutic strategies. As a marker of functionalization, the cardiomyocyte membrane allows the slow entry and excretion of sodium, calcium, and potassium ions during contraction and relaxation of the cardiomyocyte [12]. In order to maintain the physiological properties of the transplanted exogenous cells consistent with autologous myocardium, suitable conditions are required to mimic their natural environment [13]. One approach to improve the function of cardiomyocyte cultures *in vitro* is mimicking the natural electrophysiological environment. Modulated electrical stimulation is emerging as an increasingly attractive biomimetic approach, and exogenous electrical stimulation has been demonstrated to induce functional maturation of cardiomyocytes [14-16], which provides an ideal *in vitro* medium for maintaining fully functional cardiomyocytes [16, 17]. Currently, the devices used to electrically stimulate cardiomyocytes can be either signal generators or implanted cardiac pacemakers. However, both devices are limited by their bulky size and battery power, making them less portable and impractical for long-term use. Therefore, it is necessary to develop a self-powered, portable, and even implantable electrical

stimulator to provide electrical stimulation to cardiomyocytes *in vitro* and *in vivo*.

Triboelectric nanogenerator (TENG) can convert biomechanical energy into electrical energy and has the advantage of flexibility, small size, and good biocompatibility. It has been reported that TENG could convert the respiratory energy or heartbeat energy of animals into electrical energy, thereby realizing the sensing of physiological signals or as an energy source to drive cardiac pacemakers [18-20]. In addition, nanogenerator-based self-powered electrical stimulators have been demonstrated to have broad applications in tissue engineering[21, 22], including wound healing [23-26], bone repair [27-29] and cell alignment [30]. More importantly, the frequency of electric pulses generated by implantable TENG *in vivo* is consistent with the physiological rhythm of breathing or heartbeat, implying that the TENG can provide electrical stimulation with the cardiac electrophysiological rhythm compared to fixed-frequency stimulators. Taken together, TENG is a suitable candidate for self-powered and miniaturized electrical stimulator to induce functional maturation of cardiomyocytes.

In this work, we proposed a TENG-based self-powered electrical stimulation strategy for the treatment of damaged myocardium, and neonatal rat cardiomyocytes (NRCMs) were selected as model cells to study the effect of TENG on the maturation of NRCMs (Fig. 1a). The effect of different output voltages of TENG on NRCM viability was systematically investigated. Cell experiments confirmed that both the transient rate and the peak amplitude of Ca^{2+} in NRCMs increased after electrical stimulation by TENG. Further results showed that TENG-based electrical stimulation significantly promoted NRCM maturation by increasing the expression of connexin 43, α -actinin, and c-troponin T. In immature CMs, gap junctions are distributed circumferentially, while junctions in mature CMs after electrical stimulation were polarized into intercalated discs at the cell ends, leading to faster electrical conduction. In addition, TENG-based electrical stimulation also improved sarcomere organization and junction formation (Fig. 1b) and increased the intracellular Ca^{2+} levels. TENG was also demonstrated to be self-powered by the physiological movement of animals (Fig. 1c), suggesting it could be used as an implantable medical electronic device for

electrically promoting the maturation of neonatal cardiomyocytes. This work develops a TENG-based self-powered implantable medical device, which provides important technical support for clinical treatment of myocardial defects and restoration of the physiological function of cardiac tissue.

2. Materials and methods

2.1. Fabrication of the TENGs with different output voltage for NRCMs stimulation

Aluminum (Al) foils and Polytetrafluoroethylene (PTFE) films were selected as two tribo-layers of TENG and were washed with ethanol and deionized water three times before preparation. A layer of copper tape was pasted on the back of PTFE films to serve as one electrode, and the Al foil served as both electrode and another tribo-layer. To fabricate TENGs with different output voltages, tribo-layers of different sizes were cut (1 cm × 1.5 cm and 2 cm × 1.5 cm). On this basis, different microstructures were fabricated on both tribo-surfaces by adjusting sandpaper polishing methods according to previous protocols to obtain TENGs with output voltages of 5 V, 10 V, 15 V, and 20 V. Al electrode and Cu electrode were connected with copper wire by silver (Ag) paste. Then sponge tapes were attached to the back of two tribo-layers to enhance the fatigue resistance of TENG. The spacer was made of PET flexible film, keeping the PTFE film at a fixed distance away from the Al foil. The open-circuit voltage of TENG was measured by a digital phosphor oscilloscope (MSO64B 6-BW-1000), and the short current and the quantity of transferred charges were measured by an electrometer (Keithley 6517B, USA).

2.2. Fabrication of electric stimulation system based on TENG and interdigital electrodes

Interdigital electrodes were prepared by photolithography and magnetron sputtering methods, the width of the electrodes and the gap between two adjacent electrodes were 100 μ m and 300 μ m, respectively. The interdigital electrodes were spin-coated with a thin layer of PDMS film (50 μ m) to prevent itself from electrochemically reacting with the culture medium. The TENG driven by a linear motor was directly

connected to the interdigital electrodes.

2.3. Isolation and culture of NRVMs

The NRVMs were isolated from 1-day-old neonatal Sprague-Dawley (SD) rats as reported previously. Animal experiments were performed in accordance with the guidelines of the Institutional Animal Care and Use Committee of the Chinese Academy of Military Medical Science and approved by its Committee on the Ethics of Animal Experiments. The cells were pre-plated for 2 h to enrich cardiomyocytes after isolation. Then NRVMs (>90% purity) were seeded and cultured immediately in high glucose DMEM (Gibco BRL, Gaithersburg, MD, USA) containing 15% fetal bovine serum (FBS, Gibco) at 37 °C for 2 h. at 37°C, 5% CO₂. The medium was changed every 2 days.

2.4. Electrical stimulation of NRVMs

The self-powered electrical stimulation device consisted of a TENG and flexible interdigital electrodes as shown in Fig. 1. The NRVMs were attached to the interdigitated electrode. The TENG converted the mechanical energy of a linear motor with the frequency of 1 Hz, which acted as an energy source and provides an electric field (EF) that can be applied to NRVMs. The EF stimulation was performed 24 hours after seeding and was applied continuously for an additional 6 days. The group without EF treatment was the control group.

2.5. LIVE/DEAD assay

Cell cytotoxicity was analyzed using the LIVE/DEAD Viability Assay Kit (Invitrogen) according to the manufacturer's instructions. On day 4, NRVMs were stained with calcein-AM solution (LIVE)/ ethidium homodimer solution (DEAD) to detect live/dead cells respectively and incubated at 37 °C for 30 min in a 5% CO₂ incubator. NRVMs staining was analyzed under a Ti-2000 fluorescence microscope (Nikon, Japan). The number of live and dead cells in 3 randomly selected fields of each sample was analyzed by ImageJ software for all 4 samples in every group.

2.6. CCK-8 assay

Cell viability of NRVMs was analyzed using the CCK-8 assay (Abcam). On day 4, the CCK-8 reagent was added to the DMEM medium and the culture medium was changed to a 3 mL medium with CCK-8 (1:10). After 1 h of incubation, the medium with CCK-8 was added to a 96 well plate at 200 μ L/well and the medium without cells was added for blank wells. The absorbance values were measured using an enzyme-linked immunosorbent assay microplate reader and the detection wavelength was 450 nm.

2.7. Immunofluorescence Staining and Confocal Microscopy

After 4 and 7 days of cultivation, the NRVMs were fixed in 4 % formaldehyde for 30 min at room temperature. Then, the cells were permeabilized in 0.3 % Triton-100 for 30 min and blocked with 2 % goat serum for 60 min. To observe cell morphology on different hydrogels, rhodamine-phalloidin and 4',6-diamidino-2-phenylindole (DAPI) were used for F-actin nuclei staining, respectively. To evaluate the maturation of NRCMs, the cells were incubated with primary antibodies overnight at 4 °C. The following primary antibodies were used to stain cells: mouse monoclonal anti-troponin T (c-TnT, 1:200, Abcam), rabbit polyclonal anti-connexin-43 (Cx-43, 1:1000, Abcam), and mouse monoclonal anti- α -actinin (1:100, Abcam). The relative immunofluorescence Alexa Fluor 488- and Alexa Fluor 548-conjugated secondary antibodies (1:500, Abcam) were conjugated with the primary antibody for 2 h of cultivation at 37 °C. Finally, the cells were counterstained with Hoechst33258 4-6-diamidino-2-phenylindole (DAPI) (Sigma, 1:1000) and analyzed under an A1 confocal microscope (Nikon, Japan).

2.8. qRT-PCR analysis

After 4 and 7 days of cultivation, total RNA was isolated from the cells cultured in the presence or absence of EF stimulation using TRIzol reagent (Invitrogen) according to the manufacturer's instructions and used for cDNA synthesis with the SuperScript II Reverse Transcription Kit (TaKaRa, Japan). Quantitative real-time PCR (qRT-PCR) analysis was performed using SYBR Green gene expression assays (TaKaRa, Japan) with GAPDH as an internal control. The primer sequences used in

qRT-PCR are shown in Table 1. The gene expression level was calculated using the $\Delta\Delta C_t$ method (n = 3).

Table 1 The primer sequences for RT-PCR.

Gene	Primer sequence (5'–3')
Cx43	Forward: TCCTTGGTGTCTCTCGCTTT Reverse: GAGCAGCCATTGAAGTAGGC
c-TnT	Forward: GCCAGAGATGCTGAAGATGGT Reverse: GCACCAAGTTGGGCATGAAG
α -actinin (Actn1)	Forward: CGAGTGCACAAGATCTCCAA Reverse: CTCTGACACCACAGGAGCAA
Myh6	Forward: GCCCAGTACCTCCGAAAGTC Reverse: GCCTTAACATACTCCTCCTTGTC
Myh7	Forward: GCAGAAGCGCAACGCAGAGT Reverse: TGCTGCACCTTGCGGAACTTG
Nkx2.5	Forward: TTTTATCCGCGAGCCTACGG Reverse: TCTGTCTCGGCTTTGTCCAG
GAPDH	Forward: GGCATTGCTCTCAATGACAA Reverse: TGTGAGGGAGATGCTCAGTG

2.9. Western Blot Analysis

After 7 days of NRVM cultivation, Laemmli Sample Buffer (Bio-Rad) was used to lyse the proteins, and the BCATM Protein Assay Kit (Thermo Scientific) was used to determine the concentration of the extracted proteins. Then, 60 mg of proteins were electrophoresed by SDS-PAGE and transferred to a PVDF membrane (Millipore, Corporation, MA) for detection of the target proteins: Cx-43 (1:3000, Abcam). The housekeeping GAPDH (1:2000, Abcam) was detected as a normalized control. After washing, the membranes were incubated with the appropriate HRP-conjugated secondary antibodies (1:2000, Invitrogen) and labeled proteins were visualized using the ECL chemiluminescence reagent. The band intensities were analyzed with ImageJ software.

2.10. Measurement of intracellular Ca^{2+}

Calcium indicator Fluo-4 AM was utilized to assess the level of intracellular Ca^{2+} and intracellular calcium transient of cardiomyocytes after EF stimulation. All

samples on day 5 were gently washed three times with DMEM and incubated in 10 mM fluo-4 AM (Invitrogen) and 0.1% Pluronic F-127 (Sigma-Aldrich) at 37°C for 30 minutes. The cells were gently washed three times and then incubated for another 10 min in DMEM followed by calcium transient imaging. Intracellular calcium fluorescence was analyzed under a fluorescent microscope at the 488 nm wavelength. Fluorescence changes were measured as the ratio of the fluorescent dye intensity (F) during cells' contractions over the initial background fluorescence intensity (F_0) and plotted over time.

To evaluate the level of intracellular Ca^{2+} , NRVMs were detached by 0.05% trypsin/EDTA after incubation of Fluo-4 AM. Then the mixture was centrifuged for 7 min at 1200 rpm/min, and the acquired supernatant was discarded. NRVMs were washed three times and resuspended by 1 mL PBS, Flow Cytometer was used to measure the fluorescence intensity at the excitation wavelength of 488 nm.

2.11. Implantation and electrical measurement of TENG *in vivo*

Japanese big-ear rabbit (male, 2.0 kg) and Sprague–Dawley (SD) rats (male, 180–200 g) were used for this research, All the implantation operations were approved by the Animal Research Ethics Committee of Military Medical Science, Chinese Academy of Sciences. The rats were anesthetized by intraperitoneal injection of 2% sodium pentobarbital. The rabbits were anesthetized with an intravenous injection of 3% pentobarbital sodium (30 mg/kg). The implantable TENG with different sizes were packaged as shown in Fig. 7a and sterilized by ultraviolet radiation and 75% alcohol immersion. The small encapsulated TENG (1.5 cm×2.0 cm) was implanted between the lung and diaphragm in SD rats, and the large encapsulated TENG (3 cm×2.0 cm) was implanted and attached to the heart of rabbits. The generated electrical output performance was recorded by a digital oscilloscope system (MSO64B 6-BW-1000).

2.12. Statistical analysis

GraphPad Prism9 and Microsoft Excel software were applied to evaluate statistical differences between different groups. Statistical significance was analyzed with

one-way analysis of variance (ANOVA) test or two-way analysis of variance (TNOVA) test followed by Tukey's post hoc test, and $P < 0.05$ was considered significant (* $P < 0.05$, ** $P < 0.01$, *** $P < 0.001$ and **** $P < 0.0001$).

3. Results and discussion

Plenty of research has demonstrated that exogenous electrical stimulation can induce the functional maturation of cardiac myocytes and engineered heart tissue. The output performance of TENG used in this work has the characteristics of high voltage and low current[31], which make it suitable as a power source to generate electric field stimulation. Considering the movements of the heart and lungs are all relaxation/contraction in the biological system, for TENG attached to the surface of the organ, TENGs with contact/separation mode tends to be consistent with the relaxation/contraction of the organ in direction and movement mode, which is more convenient to harvest the energy from heartbeat and breath.[22, 32-34] Therefore, in this work, a TENG with contact/separation mode was used for building an *in vitro* cardiomyocyte electrical field stimulation system, which was shown in Fig. 1a, it is mainly composed of two parts, electric stimulation source (TENG) and electric field stimulation bioreactor (interdigitated electrode). Previous works concluded that biphasic electrical field stimulation was more effective than monophasic stimulation in improving the electrical excitability of cardiac organoids[35], hence, the TENG was directly connected to the flexible interdigital electrode without rectification. The TENG used for cardiomyocyte stimulation mainly consisted of two parts: the tribo-layers and the electrode-layers. Tribo-layers were made of aluminum (Al) foil and Poly tetra fluoroethylene (PTFE) film with distinct electron-attracting abilities. A layer of copper (Cu) tape was attached on the back of PTFE film served as one electrode, and the Al foil served as both electrode and another tribo-layer. The flexible interdigital electrode used in this work is to provide cardiomyocytes with a uniform electric field. Au interdigital electrodes were prepared on the PET substrate through photo etching technique and magnetron sputtering methods, besides, a thin layer of 50 μm thick poly(dimethylsiloxane) (PDMS) film was spin-coated on Au interdigital

electrode to avoid electrochemical reaction between electrodes and culture medium. The width of the Au interdigital electrodes was 100 μm and the space between two adjacent electrodes was 300 μm . Monolayer cultures of primary neonatal rat ventricular cardiomyocytes (NRVCMs) are frequently employed model to study the functional performance of engineered cardiac tissue[36], here, NRVCMs were chosen as model cells to study the effect of TENG on myocardial tissue repair, which can be used for live imaging, immunohistochemistry, gene expression analysis and so on. The schematic diagram of cardiomyocytes under electric field stimulation induced by TENG on the packaged interdigitated electrode is shown in the lower right corner of Fig. 1a.

During the fabrication process of TENG, varieties of nano/micro patterns were produced on the TENG's tribo-surfaces to increase the friction area and improve the output performance of TENG. In this work, both tribo-surfaces of TENG were polished with sandpapers to obtain dense and homogeneous linear microgrooves, the average width of the linear microstructures was about several microns (Fig. 2a). The detailed working principle of the TENG with the vertical contact-separation mode was previously reported and shown in Fig. 2b. In the initial state, no charge was generated on both tribo-surfaces. As an external force was applied to TENG, two tribo-surfaces of TENGs were contacted and rubbed with each other, which make them oppositely charged (i.e. PTFE tribo-surface: negatively charged; Al tribo-surface: positively charged) because of their different electron-attracting abilities. Once the external force disappeared, two tribo-layers were separated subsequently, to balance the electric potential difference established by the tribo-charges on both tribo-surfaces, and free electrons in the electrodes (Al and Cu) were driven to flow back and forth through the external circuit. Therefore, free electrons flow back and forth during the TENG was periodically pressed and released, leading to the generation of the alternative current pulse.

We can learn from previous studies that pulsed alternating current (AC) stimulation was effective for the maturation of neonatal rat cardiomyocytes. According to previous works, the output voltages of TENG implanted *in vivo* are driven by

respiration or heartbeat ranging from a few volts to tens of volts. In this work, four TENGs with different out voltages (5 V, 10 V, 15 V, and 20V) were fabricated to investigate the relationship between the electric field intensity induced by TENG and the functional performance of NRVCMs. According to previous studies and the principle of TENG, the output performance of TENG depends on many factors, including the size of tribo-surface of TENG[37], the density of triboelectric charge at the contact interface between the two friction materials[38], different microstructures fabricated on tribo-surfaces and the distance of the two friction-layers[39, 40]. In this work, TENG with different out voltages were fabricated by changing the size and microstructures on tribo-surfaces and driven by a linear motor[41]. The open-circuit voltage waveforms and the enlarged waveforms of the four TENGs were shown in Fig. 2c and Fig. 2d, and the working frequency of the four TENGs was 1 Hz. Besides, the short-circuit current and transferred charge waveforms of the four TENGs were also recorded and shown in Fig. S1. Four TENGs with different output voltages all showed good stability after being tested continuously for more than 14 days (Fig. 2e and Fig. S2). During the process of stimulating of NRVCMs with electric fields generated by the four TENGs mentioned above, the voltages applied to interdigital electrode were 0.6 V, 1.2 V, 1.8 V and 2.4 V, respectively (Fig. S3). Considering the width of the Au interdigital electrodes, the space between two adjacent electrodes, and the thickness of the PDMS package layer, the actual strength of electric field (EF) applied on NRVCMs generated from TENG and interdigital electrode was about 20 V/cm, 40 V/cm, 60 V/cm and 80 V/cm (Fig. 2f), and the stimulate depth was about 100-400 μm (Fig. S4). All the numerical values calculated by COMSOL Multiphysics software were shown in Fig. 2g.

To evaluate the biocompatibility of EF stimulation generated by TENG with different voltages and to determine the optimal parameters for NRVCMs cultivation, LIVE/DEAD staining, and the cell counting kit 8 (CCK8) assay were carried out on day 4 after being stimulated for 3 days. The LIVE/DEAD staining (Fig. 3a and Fig. 3b) showed that there was no significant difference in viability of NRVCMs between the 5 V and 10 V EF stimulation groups and the 0 V control group. On the contrary, the

viability of NRVCMs stimulated by higher EF stimulation voltages (15 V and 20 V) was significantly lower than NRVCMs in the control group. The CCK-8 assay (Fig. 3c) showed no significant difference in proliferation rate between the EF stimulation groups and the control group. Considering the cell viability of NRVCMs in higher EF stimulation groups (15 V and 20 V) had a downward trend compared with the control group, TENGs with output voltages of 5 V and 10 V were chosen for further research.

NRVCMs are characterized by their rhythmic beating and contractile forces, which are related to functional maturation and are triggered by intracellular calcium signals. Therefore, in order to investigate the modulatory effect of EF stimulation generated by TENG on the performance of NRVCMs, the spontaneous intracellular Ca^{2+} transients were measured using a fluorescent calcium indicator (Fluo 4 AM) by video recording. In Fig.4 (a, b and c), three representative traces of spontaneous Ca^{2+} oscillations in each NRVCMs group (control group, 5 V group and 10 V group) were selected to be shown. In Fig. 4a (i.e. control group), interval times of spontaneous Ca^{2+} oscillations were a few seconds, and the amplitudes of spontaneous Ca^{2+} oscillations were low. In Fig. 4b (i.e. 5 V group), the amplitudes and frequency of spontaneous Ca^{2+} oscillations were slightly higher than that in control group, besides, more uniform, stable rhythmic Ca^{2+} oscillations were exhibited. In Fig. 4c (i.e. 10 V group), the amplitudes of spontaneous Ca^{2+} oscillations were improved obviously and the Ca^{2+} transients rate was slightly improved compared with those in 5 V group. Overall, the Ca^{2+} transient rate and Ca^{2+} peak amplitudes showed an increasing trend with increasing voltages (Fig. 4d-e). In previous studies, researchers have demonstrated that the magnitude of force generation and maturation of calcium dynamics in CMs correlate with the magnitude and rate of the Ca^{2+} transient [36, 42]. These results preliminarily indicated that the contractile and electrophysiological performance of NRVCMs can be enhanced by EF stimulation generated by TENG, more experiments were carried out to further demonstrated the above conclusion.

The changes in cell functions are also reflected in alterations in cell morphology. To evaluate the effects of EF stimulation generated by TENG on the phenotype of NRVCMs, the rhodamine-phalloidin staining was carried out on day 4 and day 7 (Fig.

S5). It was found that the difference between 5V and 10V experiments was not obvious, but it was noticeable that the morphology of NRVCMs with 5 V and 10 V EF stimulation was different from that in the control group on day 7, the former exhibited more elongation and thicker actin filaments compared to the latter. These experiments show that the EF stimulation generated by TENG could promote the formation of NRVCMs with better organization.

Considering the strong electric conduction and contraction of NRVCMs. The effect of EF stimulation on the electrophysiological- and mechanical properties of NRVCMs should be assessed. We then measured the variation of connexin-43 (Cx43), and troponin T (cTnT) by immunofluorescence staining on day 4 and day 7. The Cx43 is an intercalated discs related protein that forms gap junction channels and can regulate electrical signal propagation between NRVCMs, and cTnT is a cardiac-specific contractile protein of myofilament reassembly in rat cardiomyocytes. Immunofluorescence staining showed that Cx43 was upregulated and had a trend of increased accumulation in EF stimulation groups compared to that in the control group on day 4 (Fig. S6) and day 7 (Fig. 5a-c). On day 7, Cx43 was dispersed in the cytoplasm and cytomembrane as a mottled pattern in the control group, but in the EF stimulation groups, Cx43 appeared to specifically gather in a linear distribution between adjacent cells, where they could perform their electrical conduction function. Western blotting provided further evidence that NRVCMs in the EF stimulation groups had a significant increase in Cx43 expression compared with that in the control group (Fig. S7), which was consistent with the observation of confocal microscopy. All the results implied that EF stimulation generated by TENG could promote the expression and assembly of electrical and mechanical proteins of NRVCMs.

In addition, qRT-PCR was performed to analyze the expression levels of cardiomyocyte-specific markers (Cx43, cTnT, α -actinin, Myh6, Myh7, and Nkx2.5) in both groups (control and EF stimulation). The expression level of Cx43 in the EF stimulation groups was significantly higher than those in the control group on day 4 and day 7 (Fig. 5d), which was consistent with the results of immunofluorescence

staining and western blotting, suggesting the improvement of electrophysiological properties of NRVCMs. Apart from that, the expression levels of cardiomyocyte markers (cTnT, α -actinin, and Myh6) in the EF stimulation groups were significantly higher than those in the control group on day 4 and day 7 (Fig. 5e-g). Both cTnT and α -actinin are common cardiac-specific contractile genes in cardiomyocytes. Besides, Myh6 is an essential sarcomere gene, which encodes myosin heavy chain α (α -HMC), and α -HMC is also a mature and contractile marker of cardiomyocytes. The increase of cTnT, α -actinin, and Myh6 expression levels in EF stimulation groups suggests the enhancement of mechanical properties of NRVCMs after EF stimulation. Moreover, the expression levels of Myh7 and Nkx2.5 in the 10 V group were higher than those in the control group on day 7 (Fig. 5h-i). The increase in the expression of the two cardiomyocyte-specific markers further indicates the functional enrichment and maturation of NRVCMs induced by EF stimulation generated by TENG. Based on the observed cardiomyocyte-specific gene expression profile, it is conceivable to conclude that the EF stimulation generated by TENG might exert favorable benefits to prolong the maintenance of functional cardiomyocytes.

NRVCMs showed stronger expression of the contractility-related markers including Cx43, cTnT, α -actinin, Myh6, and Myh7 after EF stimulation generated by TENG when compared to the control group. The results demonstrated that EF stimulation generated by TENG could promote the contractility of NRVCMs. To assess the effect of EF stimulation on NRVCMs contractility and beating, we then measured the beating rate of NRVCMs by video recording analyses (Fig. 6a). Video analyses determined motion-tracking information and quantitatively investigated the different cardiomyocyte beating behavior upon EF stimulation (Supplemental Movie1-3). As illustrated in Fig. 6b, the beating rate of NRVCMs in the EF stimulation groups significantly increased compared to the control group, which indicated the maturation of contractile behavior of cardiomyocytes after EF stimulation generated by TENG (Fig. 6b). Additionally, the relationship between beating frequency of cardiomyocytes and the frequency of TENG was also investigated and shown in Fig. S8, the average beating rate of NRVCMs showed an

increasing trend with different frequency of TENG (voltage amplitude = 5 V).

We have proved the active role of EF stimulation generated by TENG in regulating the maturation and contractile function of NRVCMs, but how it works was not clear yet. It was reported that calcium is an essential messenger for cardiac excitation-contraction coupling (E-C coupling) and EF stimulation can activate the electrically sensitive Ca^{2+} signal transduction (Fig. 6c). To assess the role of calcium in the effect of EF stimulation, we measured the intracellular Ca^{2+} level of NRVCMs with and without EF stimulation by flow cytometry (Fig.S9). The intracellular Ca^{2+} level of NRVCMs was indicated by staining with Fluo-4 AM (Fig. 6d). The Ca^{2+} positive NRVCMs and the fluorescence intensity were obtained and calculated by flow cytometry. The flow cytometric histogram profiles of different groups showed the distribution of Ca^{2+} fluorescence intensity (Fig. 6e). The average fluorescence intensity of intracellular Fluo-4 (representing Ca^{2+} level) in the EF stimulation groups significantly increased compared to the control group (Fig. 6f), which implied that calcium participates in the effect of EF stimulation generated by TENG on regulating the maturation and contractile function of NRVCMs.

Based on the above results, we can conclude that TENG can effectively induce the functional maturation of cardiomyocytes. Additionally, TENG has the potential for self-powered electrically induced functional maturation of cardiomyocytes, we implanted the flexible TENG in living creatures. To enhance the structural stability and prevent tissue fluid permeation, the TENG was encapsulated with Teflon tape and a thin layer of PDMS before being implanted *in vivo*, the size of this implantable TENG is 1.5 cm × 2 cm. The schematic diagram and image of implantable TENG were shown in Fig.7a and Fig. 7d, respectively. The implantable TENG was set between lung and diaphragm, with the flexible PTFE film contacted with the lung, which can harvest the mechanical energy from the periodic dilation of the lungs during respiration, whose schematic diagram was shown in Fig. 7b. Previous works have demonstrated that injecting hydrogel with stem cells can increase cardiac ejection fraction and contractility effectively. To promote the retention of stem cells

and functional maturation of cardiomyocytes induced by stem cells after transplantation, electrical stimulation can be combined. The flexible interdigital electrode attached to the heart can produce electric field stimulation for cardiomyocytes at the myocardial infarction surface (inset in Fig. 7b). The image of the flexible interdigital electrode was shown in Fig. 7c. In this work, the possibility of practical use of the self-powered implantable TENG for promoting the maturation of cardiomyocytes was verified by implanting the flexible TENG between the lung and diaphragm of the SD rat, followed by attaching the flexible interdigital electrode on the heart of this SD rat (Fig. 7e). The frequency of voltage pulses induced by respiration was 1.5 Hz, which is within the range of commonly used parameters for electrically induced functional maturation of cardiomyocytes. The output open-circuit voltage of the implantable TENG driven by respiration was about 0.4 V (Fig. 7f), which indicates that the implantable TENG can generate voltage pulses through the rat's respiration to promote the functional maturation of cardiomyocytes.

Considering the output performance of TENG can be greatly influenced by the size, the output voltage of TENG can be limited by the small animal, another TENG with a larger size (3 cm × 2 cm) was fabricated. In addition to breath, TENG can also be driven by heartbeat by attaching it to the pericardium, therefore, an integrated device was designed by integrating the flexible TENG with the flexible interdigital electrode. The schematic diagram of the integrated device was shown in Fig. 7g, and the photograph of an integrated device with the size of 2 cm×2 cm was shown in Fig. S10. After implanting it into the Japanese big-ear rabbit and attaching it to the pericardium, the output open-circuit voltage can reach to about 2 V, and the frequency of the voltage pulses is consistent with the heart rate of rabbit (Fig. 7 h). The voltage pulses of TENGs driven by heartbeats provide EF stimulation that mimic those produced by natural heart muscle, which have the potential to induce synchronous contractions of cardiomyocytes *in vivo*[43]. The obtained output voltage value of the implantable TENG was less than 5 V in this work. Considering the higher voltage value could have a better effect on the maturation of cardiomyocytes, more efforts

should be made in future work to obtain implantable TENGs with higher output performance.

Besides the output performance, biocompatibility and stability are also two crucial properties for implantable TENGs. To investigate the biocompatibility of the implantable TENG, the encapsulated TENG was implanted between the subdermal layer and the skeletal muscle layer. Rats were grouped into sham operation (Sham), and TENG treatment (TENG). After 1 and 2 weeks, the subcutaneous tissue and muscle tissue at the implantation site were taken for histological study. As shown in Fig. S11, the hematoxylin and eosin (H&E) stained histologic section showed that there was no significant muscle damage or inflammation, suggesting that the TENG had good biocompatibility [25, 44, 45]. In addition, we have demonstrated that TENGs with different output performances show good stability after 14 days of continuous work in Fig. S2. Previous works also have proved the well encapsulated TENG showed great stability in humid or harsh environments over 30 days *in vitro*, and have validated the long-term operation of cardiac implantable nanogenerator system *in vivo* over a two-month period [44, 46]. The good stability and biocompatibility of the well encapsulated TENG were demonstrated to prove TENG has sufficient potential to be applied *in vivo* for practical application.

4. Conclusion

In summary, a self-powered electric stimulation system consisting of TENG and the interdigital electrodes was successfully fabricated, and the effects of EF stimulation generated by TENG on the functional performance of NRVCMs were studied systematically. Different strengths of electric field stimulation generated by TENGs with different output voltages were applied to NRVCMs, the output voltage of TENG should be less than 10 V, as high EF stimulation voltage may induce significant cytotoxicity to NRVCMs. After being stimulated by TENG, NRVCMs exhibited more elongation and thicker actin filaments, the expression of cardiomyocyte-specific markers (including Cx43, cTnT, α -actinin, Myh6, Myh7, and Nkx2.5), beating rate, intracellular Ca^{2+} level, Ca^{2+} transients rate and Ca^{2+} peak amplitudes all increased, all

the results demonstrated that the functional maturation of cardiomyocytes were promoted effectively. Moreover, the flexible TENGs were implanted in SD rats and Japanese big-ear rabbits and proved that they can convert mechanical energy from breath and heartbeat into electric energy or provide EF stimulation voltage directly. This work lays the foundation for TENG to be used as a self-powered electrical stimulator for providing important technical support for clinical treatment of myocardial defects and restoration of the physiological function of cardiac tissue.

Declaration of Competing Interest

The authors declare that they have no known competing financial interests or personal relationships that could have appeared to influence the work reported in this paper.

Acknowledgements

This work was supported by the National Natural Science Foundation of China (Grant Nos. 31830030), National Key Research and Development Program of China (Grant Nos. 2017YFA0106100), Joint Fund project of National Natural Science Foundation of China (Grant Nos. U21A20394), the Innovation of Science and Technology Forward 2030 program (2021ZD0201600), China National Postdoctoral Program for Innovative Talent (BX20200380).

Author Contributions

J.Z., C.W., Z.L. conceived the idea, L.M.Z. and Z.G designed the experiment. J.Z., C.W., and Z.L. guided the project. L.M.Z. fabricated the devices, L.M.Z., Z.G, W.L and C.W performed the biological experiment. L.M.Z., Z.G and W.L analyzed the data. S.C developed the theoretical models. L.M.Z. and Z.G drew the figures. L.M.Z., Z.G, D.L and S.L. prepared the manuscript. All authors discussed and reviewed the manuscript.

Reference

1. X. Yu, X. Chen, M. Amrute-Nayak, E. Allgeyer, A. Zhao, H. Chenoweth, M. Clement, J. Harrison, C. Doreth, G. Sirinakis, T. Krieg, H. Zhou, H. Huang, K. Tokuraku, D. St Johnston, Z. Mallat, X. Li, MARK4 controls ischaemic heart failure through microtubule deetyrosination. *Nature*, 594.7864 (2021): 560-565.
2. S.A. Pullano, D.C. Critello, A.S. Fiorillo, Triboelectric-induced Pseudo-ICG for cardiovascular risk assessment on flexible electronics. *Nano Energy* 67 (2020): 104278.
3. K. Zhou, Y. Xu, Q. Wang, L. Dong, Overexpression of miR-431 attenuates hypoxia/reoxygenation-induced myocardial damage via autophagy-related 3. *Acta Bioch. Bioph. Sin.* 53.2 (2021): 140-148.
4. D. Zhao, J. Zhuo, Z. Chen, J. Wu, R. Ma, X. Zhang, Y. Zhang, X. Wang, X. Wei, L. Liu, C. Pan, J. Wang, J. Yang, F. Yi, G. Yang, Eco-friendly in-situ gap generation of no-spacer triboelectric nanogenerator for monitoring cardiovascular activities. *Nano Energy* 90 (2021): 106580.
5. M.C. Alraies, P. Eckman, Adult heart transplant: indications and outcomes. *J Thorac Dis*, 6.8 (2014): 1120–1128.
6. M. Fujiwara, et al., Induction and enhancement of cardiac cell differentiation from mouse and human induced pluripotent stem cells with cyclosporin-A. *PLoS One*, 6.2 (2011): e16734.
7. S.-H. Moon, S.-W. Kang, S.-J. Park, D. Bae, S. J. Kim, H.-A. Lee, K. S. Kim, K. S. Hong, J. S. Kim, J. T. Do, K. H. Byung, H.-M. Chung, The use of aggregates of purified cardiomyocytes derived from human ESCs for functional engraftment after myocardial infarction. *Biomaterials*, 34.16 (2013): 4013-4026.
8. L. Cai, J. Xu, Z. Yang, R. Tong, Z. Dong, C. Wang, K. W. Leong, Engineered biomaterials for cancer immunotherapy. *Med. Comm*, 1.1 (2020): 35-46.
9. H. Wang, P. Agarwal, Y. Xiao, H. Peng, S. Zhao, X. Liu, S. Zhou, J. Li, Z. Liu, X. He, A Nano-In-Micro System for Enhanced Stem Cell Therapy of Ischemic Diseases, *ACS Central Sci.* 3.8 (2017): 875-885.
10. N. S. Peters, N. J. Severs, S. M. Rothery, C. Lincoln, M. H. Yacoub, C. R. Green, Spatiotemporal relation between gap junctions and fascia adherens junctions during postnatal development of human ventricular myocardium. *Circulation*, 90.2 (1994): 713-725.
11. A. P. Ziman, N. L. Gómez-Viquez, R. J. Bloch, W. J. Lederer, Excitation-contraction coupling changes during postnatal cardiac development. *J. Mol. Cell. Cardiol.*, 48.2 (2010): 379-386.
12. A. Zwartsen, T. Korte, P. Nacken, D. W. de Lange, R. H. S. Westerink, L. Hondebrink, Cardiotoxicity screening of illicit drugs and new psychoactive

substances (NPS) in human iPSC-derived cardiomyocytes using microelectrode array (MEA) recordings. *J. Mol. Cell. Cardiol.*, 136 (2019): 102-112.

13. S. Yoshida, S. Miyagawa, S. Fukushima, T. Kawamura, N. Kashiyama, F. Ohashi, T. Toyofuku, K. Toda, Y. Sawa, Maturation of Human Induced Pluripotent Stem Cell-Derived Cardiomyocytes by Soluble Factors from Human Mesenchymal Stem Cells. *Mol. Ther.*, 26.11 (2018): 2681-2695.

14. R. S. R. M. Martherus, S. J. V. Vanherle, E. D. J. Timmer, V. A. Zeijlemaker, J. L. Broers, H. J. Smeets, J. P. Geraedts, T. A. Y. Ayoubi, Electrical signals affect the cardiomyocyte transcriptome independently of contraction. *Physiol Genomics*, 42.4 (2010): 283-289.

15. W. L. Stoppel, D. L. Kaplan, L.D. Black, 3rd, Electrical and mechanical stimulation of cardiac cells and tissue constructs. *Adv. Drug Deliv. Rev.*, 96 (2016): 135-155..

16. M.N. Hirt, et al., Functional improvement and maturation of rat and human engineered heart tissue by chronic electrical stimulation. *J. Mol. Cell. Cardiol.*, 74 (2014): 151-161.

17. A. Llucià-Valldeperas, B. Sanchez, C. Soler-Botija, C. Gálvez-Montón, S. Roura, C. Prat-Vidal, I. Perea-Gil, J. Rosell-Ferrer, R. Bragos, A. Bayes-Genis, Physiological conditioning by electric field stimulation promotes cardiomyogenic gene expression in human cardiomyocyte progenitor cells. *Stem Cell Res. Ther.*, 5.4 (2014): 1-5.

18. Q. Zheng, B. Shi, F. Fan, X. Wang, L. Yan, W. Yuan, S. Wang, H. Liu, Z. Li, Z. L. Wang, *In vivo* powering of pacemaker by breathing-driven implanted triboelectric nanogenerator. *Adv. Mater.*, 26.33 (2014): 5851-5856.

19. Q. Zheng, H. Zhang, B. Shi, X. Xue, Z. Liu, Y. Jin, Y. Ma, Y. Zou, X. Wang, Z. An, W. Tang, W. Zhang, F. Yang, Y. Liu, X. Lang, Z. Xu, Z. Li, Z. L. Wang, *In vivo* self-powered wireless cardiac monitoring via implantable triboelectric nanogenerator. *ACS nano*, 10.7 (2016): 6510-6518.

20. Y. Ma, Q. Zheng, Y. Liu, B. Shi, X. Xue, W. Ji, Z. Liu, Y. Jin, Y. Zou, Z. An, W. Zhang, X. Wang, W. Jiang, Z. Xu, Z. L. Wang, Z. Li, H. Zhang, Self-powered, one-stop, and multifunctional implantable triboelectric active sensor for real-time biomedical monitoring. *Nano lett.*, 16.10 (2016): 6042-6051.

21. G. Conta, A. Libanori, T. Tat, G. Chen, J. Chen, Triboelectric Nanogenerators for Therapeutic Electrical Stimulation. *Adv. Mater.* 33.26 (2021): 2007502.

22. W. Zhang, G. Li, B. Wang, Q. Zhu, L. Zeng, Z. Wen, C. Yang, Yue Pan, Triboelectric Nanogenerators for Cellular Bioelectrical Stimulation. *Adv. Func. Mater.* (2022): 2203029.

23. Q. Guan, Y. Dai, Y. Yang, X. Bi, Z. Wen, Y. Pan, Near-infrared irradiation induced remote and efficient self-healable triboelectric nanogenerator for potential implantable electronics. *Nano Energy*, 51 (2018): 333-339.

24. W. Hu, X. Wei, L. Zhu, D. Yin, A. Wei, X. Bi, T. Liu, G. Zhou, Y. Qiang, X. Sun, Z. Wen, Y. Pan, Enhancing proliferation and migration of fibroblast cells by electric stimulation based on triboelectric nanogenerator. *Nano Energy*, 57 (2019): 600-607.
25. Z. Li, H. Feng, Q. Zheng, H. Li, C. Zhao, H. Ouyang, S. Noreena, M. Yu, F. Su, R. Liu, L. Li, Z. L. Wang, Z. Li, Photothermally tunable biodegradation of implantable triboelectric nanogenerators for tissue repairing. *Nano Energy* 54 (2018): 390-399.
26. Y. Long, H. Wei, J. Li, G. Yao, B. Yu, D. Ni, A. LF Gibson, X. Lan, Y. Jiang, W. Cai, and X. Wang. Effective Wound Healing Enabled by Discrete Alternative Electric Fields from Wearable Nanogenerators. *ACS nano* 12.12 (2018): 12533-12540.
27. J. Tian, R. Shi, Z. Liu, H. Ouyang, M. Yue, C. Zhao, Y. Zou, D. Jiang, J. Zhang, Z. Li, Self-powered implantable electrical stimulator for osteoblasts' proliferation and differentiation. *Nano Energy* 59 (2019): 705-714.
28. B. Ma, F. Liu, Z. Li, J. Duan, Y. Kong, M. Hao, S. Ge, H. Jiang, H. Liu, Piezoelectric nylon-11 nanoparticles with ultrasound assistance for high-efficiency promotion of stem cell osteogenic differentiation, *J. Mater. Chem. B*, 7.11 (2019): 1847-1854.
29. G. Li, Q. Zhu, B. Wang, R. Luo, X. Xiao, Y. Zhang, L. Ma, X. Feng, J. Huang, X. Sun, Z. Wen, Y. Pan, C. Yang, Rejuvenation of senescent bone marrow mesenchymal stromal cells by pulsed triboelectric stimulation. *Adv. Sci.* 8.18 (2021): 2100964.
30. Q. Zheng, Y. Zou, Y. Zhang, Z. Liu, B. Shi, X. Wang, Y. Jin, H. Ouyang, Z. Li, Z. L. Wang, Biodegradable triboelectric nanogenerator as a life-time designed implantable power source. *Sci. Adv.* 2.3 (2016): e1501478.
31. F.-R. Fan, Z.-Q. Tian, Z. L. Wang, Flexible triboelectric generator. *Nano energy* 1.2 (2012): 328-334.
32. B. Shi, Z. Li, Y. Fan, Implantable energy-harvesting devices, *Adv. Mater.* 30.44 (2018): 1801511.
33. Z. Liu, H. Li, B. Shi, Y. Fan, Z. L. Wang, Z. Li, Wearable and Implantable Triboelectric Nanogenerators, *Adv. Func. Mater.* 29.20 (2019): 1808820.
34. H. Ouyang, Z. Liu, N. Li, B. Shi, Y. Zou, F. Xie, Y. Ma, Z. Li, H. Li, Q. Zheng, X. Qu, Y. Fan, Z. L. Wang, H. Zhang, Z. Li, Symbiotic cardiac pacemaker. *Nat. Commun.* 10.1 (2019): 1-10.
35. L. L.Y. Chiu, R. K. Iyer, J.-P. King, M. Radisic, Biphasic electrical field stimulation aids in tissue engineering of multicell-type cardiac organoids. *Tissue. Eng. Pt. A*, 17.11-12 (2011): 1465-1477.
36. J. G. Jacot, A.D. McCulloch, J.H. Omens, Substrate stiffness affects the functional maturation of neonatal rat ventricular myocytes. *Biophys. J.* 95.7 (2008): 3479-3487.
37. X. Chen, T. Jiang, Y. Yao, L. Xu, Z. Zhao, Z. L. Wang, Stimulating Acrylic Elastomers by a Triboelectric Nanogenerator – Toward Self-Powered Electronic Skin and Artificial Muscle. *Adv. Func. Mater.* 26.27 (2016): 4906-4913.

38. H. Y. Li, L. Su, S. Y. Kuang, C. F. Pan, G. Zhu, Z. L. Wang, Significant enhancement of triboelectric charge density by fluorinated surface modification in nanoscale for converting mechanical energy. *Adv. Func. Mater.* 25.35 (2015): 5691-5697.
39. F.-R. Fan, L. Lin, G. Zhu, W. Wu, R. Zhang, Z. L. Wang. Transparent triboelectric nanogenerators and self-powered pressure sensors based on micropatterned plastic films. *Nano Lett.*, 12.6 (2012): 3109-3114.
40. S. Niu, Z.L. Wang, Theoretical systems of triboelectric nanogenerators. *Nano Energy*, 14 (2015): 161-192.
41. L. Zhao, Q. Zheng, H. Ouyang, H. Li, L. Yan, B. Shi, Z. Li. A size-unlimited surface microstructure modification method for achieving high performance triboelectric nanogenerator. *Nano Energy*, 28 (2016): 172-178.
42. F. Zhang, K. Qu, X. Li, C. Liu, L. S. Ortiz, K. Wu, X. Wang, N. Huang, Gelatin-based hydrogels combined with electrical stimulation to modulate neonatal rat cardiomyocyte beating and promote maturation. *Bio-Des. Manuf.*, 4.1 (2021): 100-110.
43. C.-W. Hsiao, M.-Y. Bai, Y. Chang, M.-F. Chung, T.-Y. Lee, C.-T. Wu, B. Maiti, Z.-X. Liao, R.-K.Li, H.-W. Sung, Electrical coupling of isolated cardiomyocyte clusters grown on aligned conductive nanofibrous meshes for their synchronized beating. *Biomaterials*, 34.4 (2013): 1063-1072.
44. Q. Zheng, Y. Jin, Z. Liu, H. Ouyang, H. Li, B. Shi, W. Jiang, H. Zhang, Z. Li, Z. L. Wang, Robust multilayered encapsulation for high-performance triboelectric nanogenerator in harsh environment. *ACS appl. Mater. inter.*, 8.40 (2016): 26697-26703.
45. H. Ryu, H. mPark, M.-K. Kim, B. Kim, H. S. Myoung, T. Y. Kim, H.-J. Yoon, S. S. Kwak, J. Kim, T. H. Hwang, E. -K. Choi, S.-W. Kim, Self-rechargeable cardiac pacemaker system with triboelectric nanogenerators. *Nat. commun.* 12.1 (2021): 1-9.
46. J. Li, T. A. Hacker, H. Wei, Y. Long, F Yang, D Ni, A. Rodgers, W. Cai, X. Wang, Long-term in vivo operation of implanted cardiac nanogenerators in swine. *Nano Energy* 90 (2021): 106507.

Figures

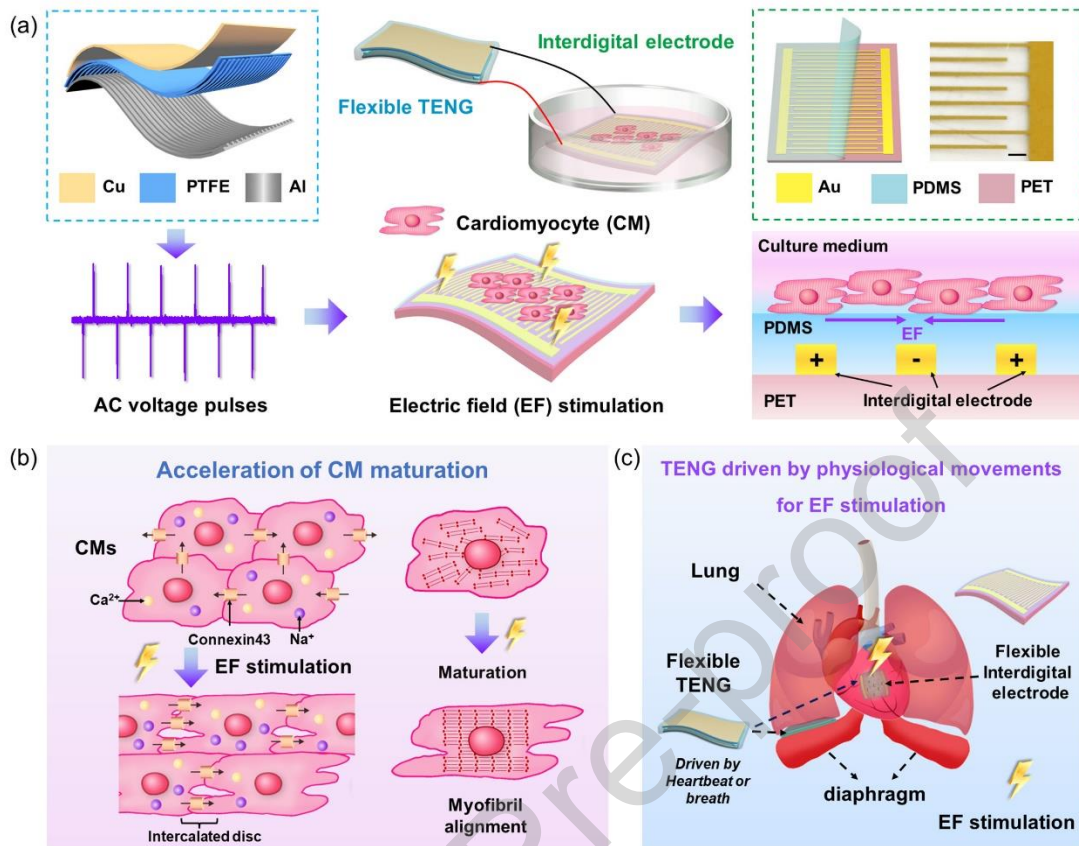


Fig.1 Schematic illustration of self-powered electric stimulator and interdigitated electrode for promoting maturation of cardiomyocyte. (a) The schematic diagram of the cardiomyocyte stimulation system *in vitro* shows the electrical field. Scale bar: 300 μm . (EF) stimulation (generated by TENG) of cardiomyocytes on the interdigitated electrode. (b) Electrical stimulation accelerates cardiomyocyte maturation. (c) Schematic of the implanted flexible TENG driven by physiological movements for EF stimulation.

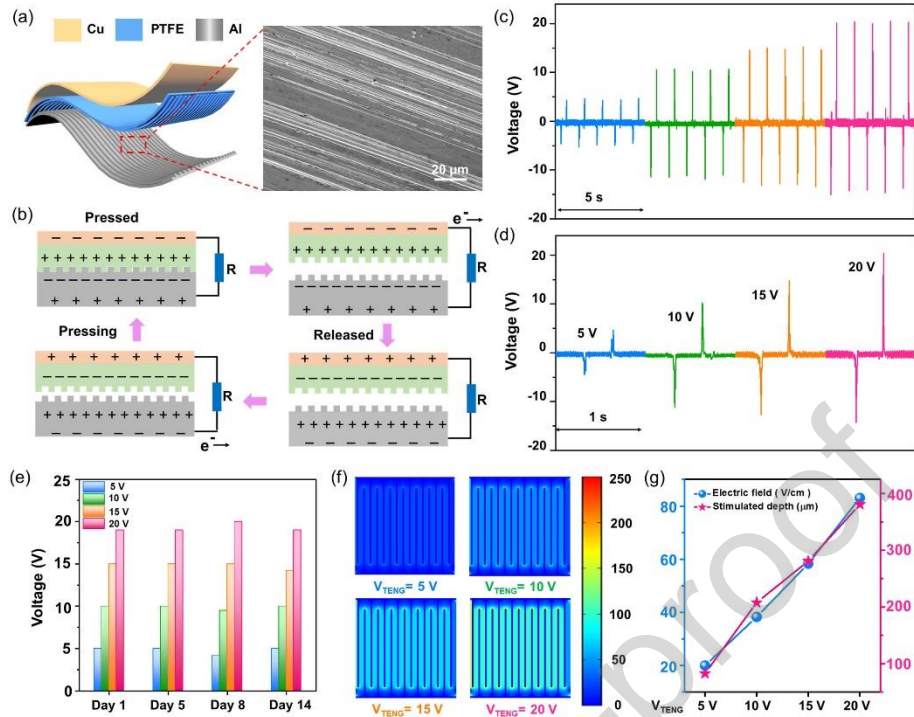


Fig. 2 The working mechanism and output performance of TENGs with different voltage and different electric field (EF) intensities generated on the packaged interdigitated electrode. (a) Schematic diagram of TENG. Inset: SEM image of the linear micro-structures on Al surface polished by sandpapers. (b) The working mechanism of the TENG. (c) The open-circuit voltage of TENGs with different voltages. (d) The enlarged waveforms of different output voltages in Fig. 2a. (e) Stability tests of TENGs with different voltages. (f) Calculated distribution of the EF of the stimulation device via finite element method. (g) Values of EF and EF stimulate depth of the stimulation device generated by TENGs with different out voltages.

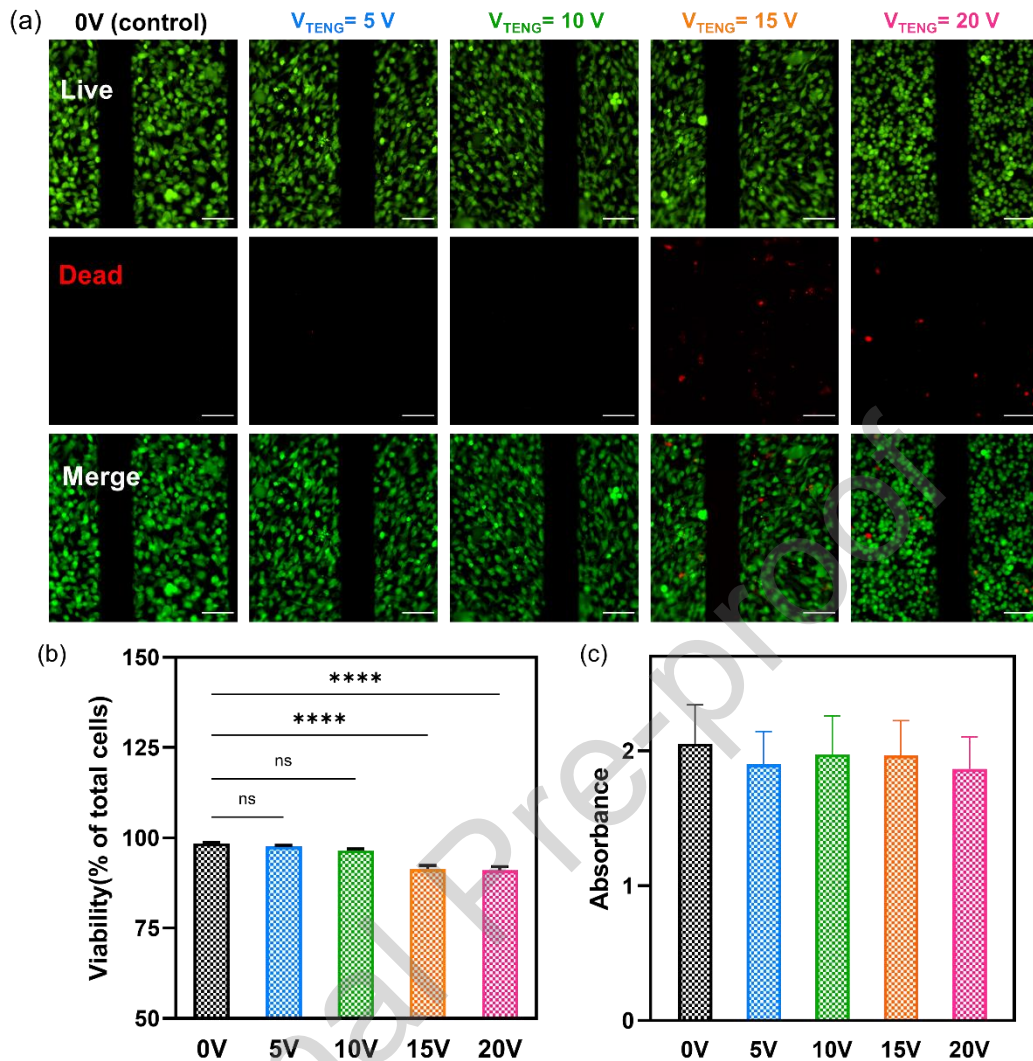


Fig.3 Growth of neonatal rat cardiomyocytes (NRVCMs) with and without EF stimulation. (a) NRVCMs stained with calcein-AM (green)/ethidium homodimer (red) after 4-day incubation with and without EF stimulation. Scale bar: 100 μ m. (b) The percentage of viable cells was statistically counted from (a) ($n = 3\sim 5$). (c) The growth and viability of NRVCMs were determined by the cell counting kit 8 (CCK8) assay ($n = 6$). Data are represented as mean \pm SEM; * $p < 0.05$, ** $p < 0.01$, *** $p < 0.001$, **** $p < 0.0001$ by one-way ANOVA analysis.

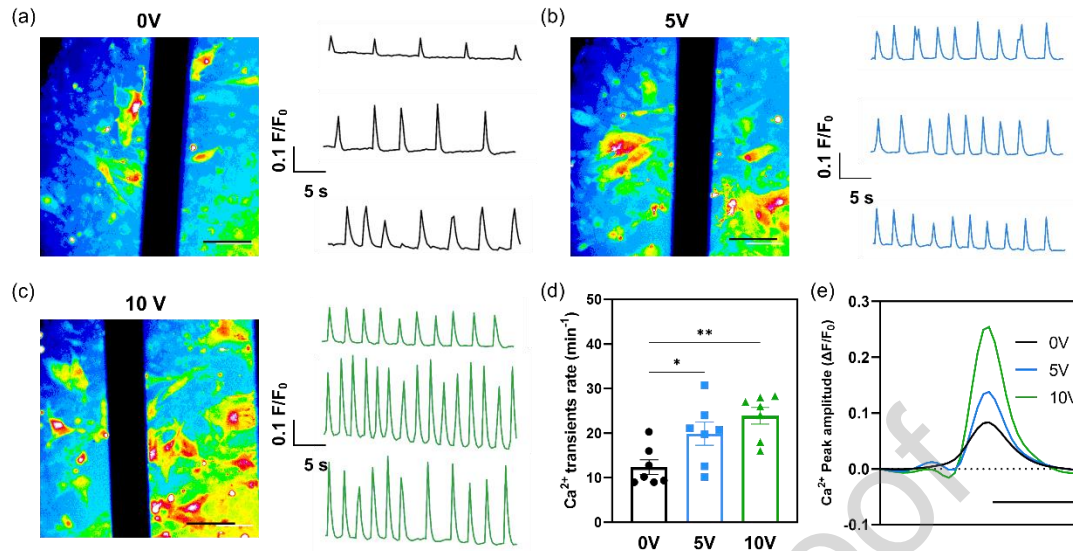


Fig. 4 Spontaneous calcium transients in NRVCMs with or without EF stimulation on days 6. (a-c) Representative confocal laser microscopy rainbow images after loading with Fluo 4 AM. Scale bars: 100 μm . Representative traces of spontaneous Ca^{2+} oscillations in NRVCMs with or without EF stimulation (Bottom). F/F_0 : change of fluorescent signal over background fluorescence. Spontaneous Ca^{2+} transients rate (d) and Ca^{2+} peak amplitudes (e) of NRVCMs with or without EF stimulation from calcium transients measurements ($n = 7$). Data are represented as mean \pm SEM; * $p < 0.05$, ** $p < 0.01$, *** $p < 0.001$ by one-way ANOVA analysis.

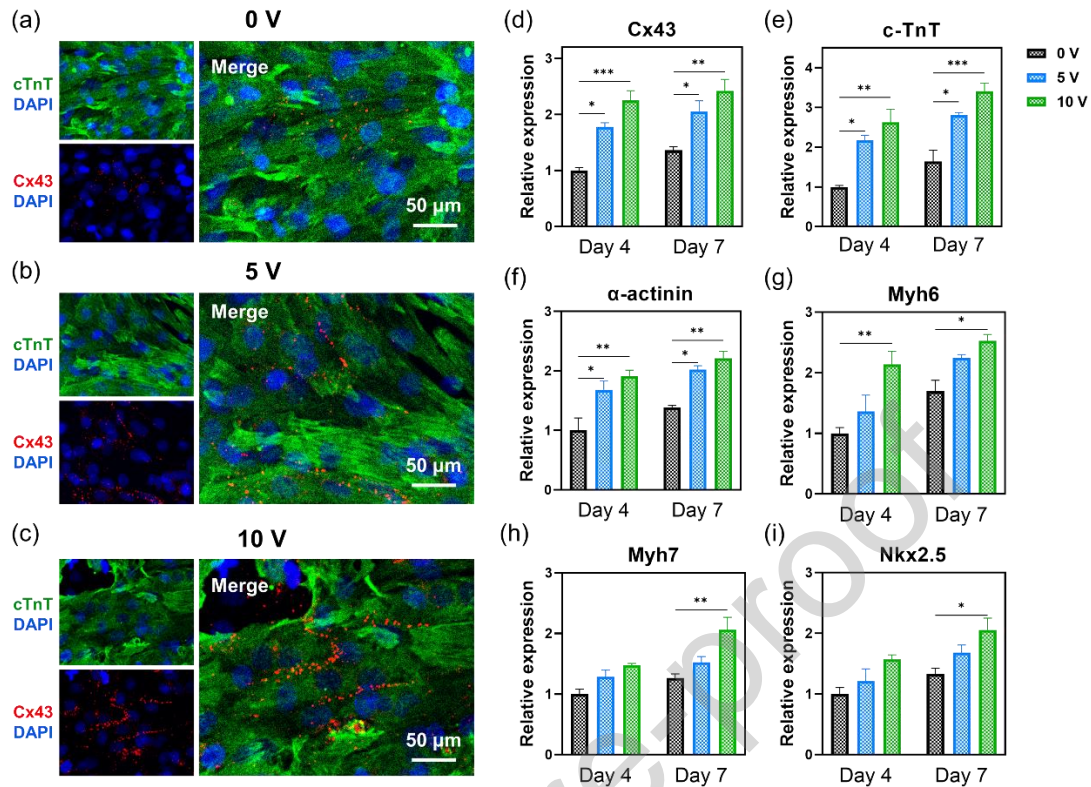


Fig. 5 Effects of EF stimulation on the phenotype and gene expression of NRVCMs after 7-day incubation. (a-c) Immunostaining of troponin T (cTnT) (green), connexin-43 (Cx43) (red) and nuclei (blue) examined by laser confocal microscopy. Scale bar: 50 μm. (d-i) Relative gene expression analysis of Cx43, c-TnT, α-actinin (Actn1), Myh6, Myh7, and Nkx2.5 from NRVCMs with or without EF stimulation by qRT-PCR (n=3). Data are represented as mean ± SEM; *p < 0.05, **p < 0.01, ***p < 0.001 by two-way analysis of variance (TNOVA) analysis.

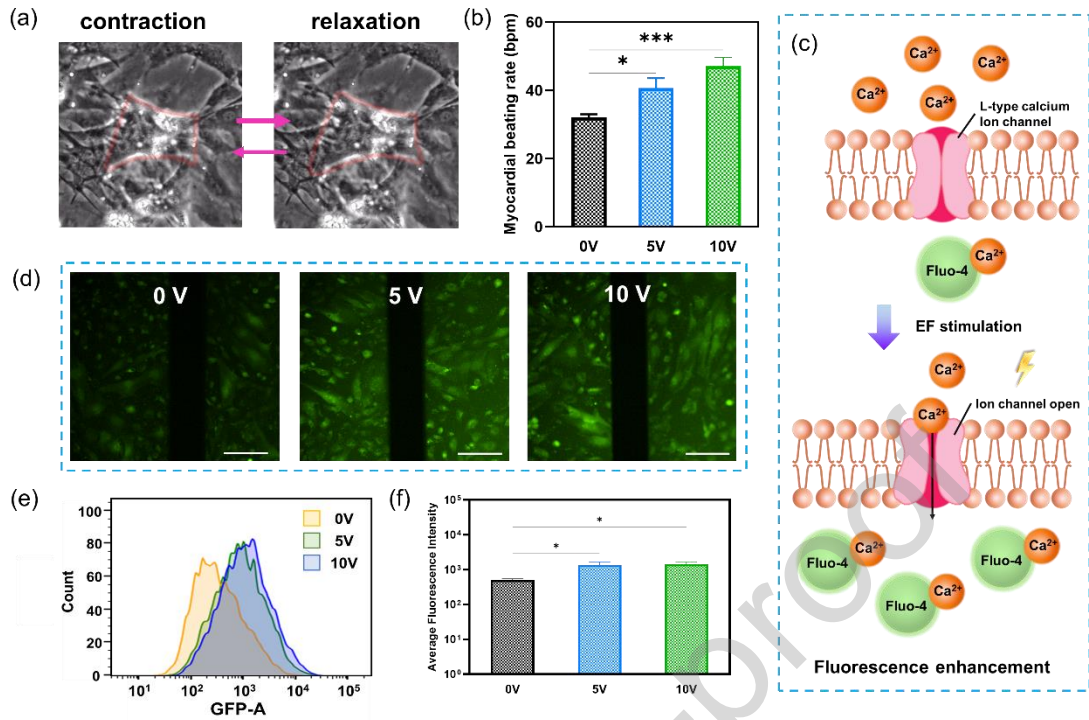


Fig. 6 Evaluation of the beating and intracellular Ca^{2+} level of NRVCMs with or without EF stimulation. (a) Representative images of the beating motions of NRVCMs during one myocardial beating cycle. Scale bars: 100 μm . (b) The myocardial beating rate of NRVCMs with or without EF stimulation ($n=7$). (c) Schematic of intracellular calcium concentration promoted by EF stimulation. (d) The optical fluorescence diagrams of NRVCMs dyed by Fluo-4 AM after EF stimulated for 6 days. Scale bar: 100 μm . (e) The single-cell distribution of fluorescence levels of NRVCMs with or without EF stimulation was measured using flow cytometry. (f) The average fluorescence intensity of NRVCMs with or without EF stimulation acquired from average GFP-A intensity by flow-cytometer. Data are represented as mean \pm SEM; * $p < 0.05$, ** $p < 0.01$, *** $p < 0.001$ by one-way ANOVA analysis.

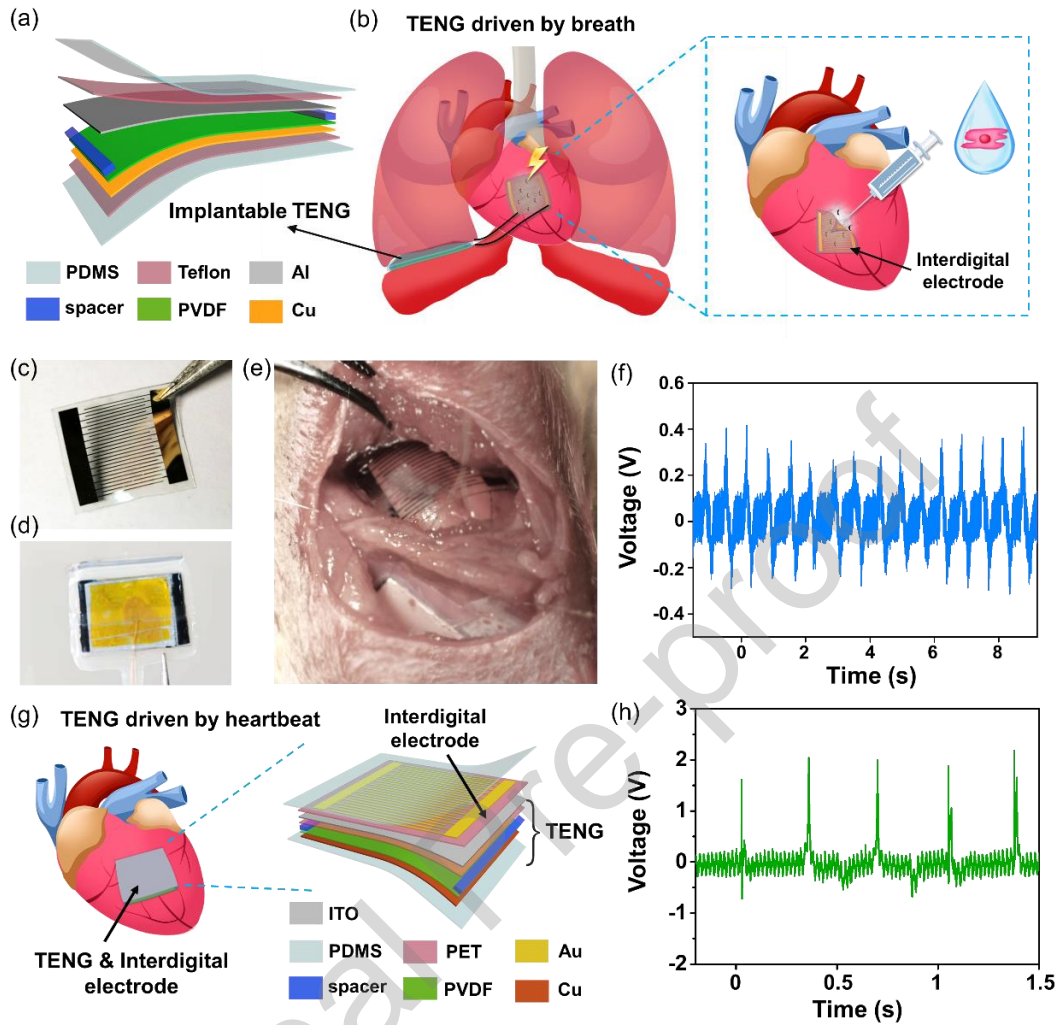


Fig. 7 The intending self-powered implantable TENG for promoting maturation of NRVCMs in vivo. (a) Schematic diagram of implantable TENG. (b) Schematic diagram of implantable TENG harvesting energy from the diaphragmatic movement for electrically induced functional maturation of cardiomyocytes injected at myocardial infarction area. (c, d) Image of implantable TENG and flexible interdigital electrode. (e) Image of implantable TENG attached to a live rat's diaphragm and a flexible interdigital electrode attached to a live rat's heart. (f) The open-circuit voltage of the implantable TENG that was attached to the rat's diaphragm. (g) Schematic diagram of implantable integrated device attached on the heart, and the structure diagram of the integrated device (TENG and interdigital electrode) (h) The output voltage of the integrated device TENG that was attached on the heart of rabbit.

Credit Author Statement

Luming Zhao: Investigation, Methodology, Writing - Original draft preparation

Zhongbao Gao: Investigation, Formal analysis, Writing- Original draft preparation.

Wei Liu: Investigation, Supervision.

Chunlan Wang: Investigation.

Dan Luo: Supervision, Writing- Original draft preparation.

Shengyu Chao: Software.

Siwei Li: Investigation.

Zhou Li: Conceptualization, Methodology, Supervision, Writing- Reviewing and Editing.

Changyong Wang: Conceptualization, Methodology, Supervision, Writing- Reviewing and Editing.

Jin Zhou: Conceptualization, Methodology, Supervision, Writing- Reviewing and Editing.

Declaration of Competing Interest

The authors declare that they have no known competing financial interests or personal relationships that could have appeared to influence the work reported in this paper.

Highlights

The highlights and innovations are as follows:

1. An effective and flexible self-powered implantable electrical stimulator based on TENG and interdigitated electrode was proposed to induce the maturation of cardiomyocytes, and the suitable range of EF stimulation strength was founded.
2. After being stimulated by TENG, both contractile and electrophysiological performance of cardiomyocytes were enhanced obviously, which demonstrated the functional maturation of cardiomyocytes.
3. The self-powered electrical stimulator was shown to work with the breath of rats and the heartbeat of rabbits, the latter result provides a potential way to induce synchronous contractions of cardiomyocytes *in vivo*.